Preformed reggie/flotillin caps: stable priming platforms for macrodomain assembly in T cells

Matthias F. Langhorst,* Alexander Reuter,* Georg Luxenhofer,*,[1] Eva-Maria Boneberg,[†] Daniel F. Legler,[†] Helmut Plattner,* and Claudia A. O. Stuermer*

*Developmental Neurobiology Group, Department of Biology, University of Konstanz, Konstanz, Germany; and [†]Biotechnology Institute Thurgau at the University of Konstanz, Tägerwilen, Switzerland

[1]Present address: Institute of Physiology, University of Hohenheim, Garbenstr. 30, D-70593 Stuttgart, Germany.

Corresponding author: Matthias Langhorst, Universitätstrasse 10, D-78457 Konstanz. E-mail: Matthiaslanghorst@email.de

ABSTRACT

T cell activation after contact with an antigen-presenting cell depends on the regulated assembly of the T cell receptor signaling complex, which involves the polarized assembly of a stable, raft-like macrodomain surrounding engaged T cell receptors. Here we show that the preformed reggie/flotillin caps present in resting T cells act as priming platforms for macrodomain assembly. Preformed reggie-1/flotillin-2 caps are exceptionally stable, as shown by fluorescence recovery after photobleaching (FRAP). Upon T cell stimulation, signaling molecules are recruited to the stable reggie/flotillin caps. Importantly, a trans-negative reggie-1/flotillin-2 deletion mutant, which interferes with assembly of the preformed reggie/flotillin cap, impairs raft polarization and macrodomain formation after T cell activation. Accordingly, expression of the trans-negative reggie-1 mutant leads to the incorrect positioning of the guanine nucleotide exchange factor Vav, resulting in defects in cytoskeletal reorganization. Thus, the preformed reggie/flotillin caps are stable priming platforms for the assembly of multiprotein complexes controlling actin reorganization during T cell activation.

Key words: lipid rafts • signal transduction • T cell activation • actin cytoskeleton • raft clustering

Membrane microdomains/lipid rafts are considered as sites for protein sorting and assembly of signaling complexes. Thus, they allow the spatio-temporal regulation of protein–protein interaction and signal transduction (1, 2). The concept of lipid rafts controlling signal transduction at the plasma membrane has largely evolved from work on lymphocyte activation (3). Lateral segregation of signaling molecules by regulated aggregation of lipid rafts is thought to control the assembly of large immune receptor signaling complexes and to regulate signal strength and duration (4, 5). Essential components of the T cell receptor (TCR) signaling complex, including LAT (linker of activated T cells), lck, fyn and the

coreceptors CD4/CD8 acquire raft affinity through palmitoylations. Their targeting to lipid rafts was shown to be crucial for efficient coupling of TCR engagement to downstream effectors (6–9).

Specific aspects of lipid rafts, such as dimension and lifetime, are still controversial (10). Moreover, the use of a variety of methods to isolate rafts, as well as different definitions of lipid rafts, raise many open questions (11, 12). Recent reports argued that lipid rafts in resting cells are small, dynamic entities unsuitable to act as signaling scaffolds (13, 14). Furthermore, different types of lipid microdomains exist on the single cell level, as evidenced by the segregation of GM1-and GM3-enriched membrane domains during T cell polarization and migration (15). Activation of T cells, however, triggers the formation of stable macrodomains/clustered rafts around the engaged TCR complex (3, 16, 17), as was recently unambiguously shown by visualizing directly the order of the membrane in the vicinity of engaged TCRs using the fluorescent dye Laurdan (18). Macrodomain assembly is regulated by extensive actin cytoskeleton remodeling (16, 18–21) and is further enhanced by costimulation (18, 22).

Reggie-1 and -2 were discovered in our lab as proteins upregulated in retinal ganglion cells during regeneration of lesioned axons in the goldfish optic nerve (23, 24). They were independently described as components of detergent-insoluble, "floating" fractions from murine lung tissue and accordingly named flotillin-2 and flotillin-1, respectively (25). Both reggies localize at the cytoplasmic leaflet of the plasma membrane and associate with lipid rafts via multiple palmitoylations. Additionally, reggie-1 is myristoylated (26, 27). The reggies form homo-oligomers and probably hetero-oligomers via their C terminus, which contains several α-helical EA-repeats predicted to form coiled coils (25, 26). Their precise cellular function remains enigmatic, but they probably act as oligomeric scaffolding proteins for multiprotein complex assembly (reviewed in (28)).

Reggies often form clusters of 50–100 nm at the plasma membrane of resting cells (29, 30). In lymphocytes, these clusters are asymmetrically distributed, accumulating in one aspect of the cell building a preformed cap (31). These preformed reggie caps confer a general polarity to resting lymphocytes, which are widely considered as unpolarized before stimulation. In T lymphocytes, reggies are closely associated with the Src family kinases lck and fyn and the adaptor protein LAT, as shown by coimmunoprecipitation assays and colocalization experiments at the light and electron microscopic level (29, 30, 32, 33). Cell activation by cross-linking of surface molecules leads to the accumulation of important components of the TCR signaling complex, including CD3, LAT, and lck in the region of the reggie caps (30, 31). This is reflected by an increased biochemical association of for example, LAT and lck with the reggies (32, 33).

Using fluorescence recovery after photobleaching (FRAP), we show in the present study that the preformed reggie caps are exceptionally stable structures, both in resting and activated T cells. We generated a trans-negative reggie-1 deletion mutant, which interferes with the assembly of the preformed reggie caps. Expression of this mutant inhibits macrodomain assembly after T cell activation and impairs stimulation-induced T cell spreading but does not influence ERK1/2 activation or Ca^{2+}-signaling. Reggie-1 associates with Vav, and interfering with reggie-1 function leads to a mislocalization of Vav during spreading. Thus, the preformed reggie caps are stable platforms for multiprotein complexes controlling actin reorganization during T cell activation.

MATERIALS AND METHODS

Antibodies, plasmids, and reagents

Anti-reggie-1 (anti-ESA/flotillin-2) and anti-reggie-2 (flotillin-1) monoclonal antibodies (mAB) were obtained from BD Transduction Laboratories (Heidelberg, Germany); anti-lck, anti-LAT and goat-anti-mouse-Alexa 488 polyclonal antibodies were obtained from Biomol (Hamburg, Germany); anti-EGFP was obtained from Clontech (Heidelberg, Germany); anti-Vav polyclonal antibody was obtained from Santa Cruz Biotechnology (Santa Cruz, CA); anti-phospho-ZAP70 (Tyr319), anti-phospho-ERK1/2 (Thr 202/Tyr 204), and anti-ERK1/2 polyclonal antibodies were obtained from Cell Signaling (Beverly, MA); and donkey-anti-mouse-Cy3 was obtained from Jackson ImmunoResearch (Soham, UK).

Rat reggie-1 full-length cloned into pEGFP-N1 (Clontech) was a kind gift from R. Tikkanen (Frankfurt, Germany). The deletion mutants R1L1, lacking the C-terminal half of the protein (aa 278-428), and R1EA, lacking both the N-terminal half of the protein (aa 1-183) and the extreme C terminus (aa 391-428), were amplified by PCR using full-length rat reggie-1 as a template, and primers introducing restriction sites for *Eco*RI and *Bam*HI. PCR fragments were subcloned into pEGFP-N1 and pDsRed2-C1 (Clontech), respectively.

Concanavalin A (ConA), cytochalasin D, and latrunculin A were purchased from Calbiochem (Bad Soden, Germany), poly-L-lysine and methyl-β-cyclodextrin from Sigma (Munich, Germany), *Staphylococcus* enterotoxin E (SEE) from Alexis (Gruenberg, Germany). Phalloidin-Alexa 568, Concanavalin A-Alexa 568, cholera toxin-Alexa 555, and Fluo4-AM were from Molecular Probes (Leiden, Netherlands).

Cell culture and transfection

Jurkat T lymphocytes were maintained as described previously (30) and were transfected by electroporation using a BTX 600 Electro Cell Manipulator, according to the manufacturer's instructions. Raji B lymphocytes were a kind gift from E. May (Konstanz) and were cultured as Jurkat T cells. PC12 cells were maintained in DMEM supplemented with 10% FCS, 100 units/ml penicillin, 50 mg/ml streptomycin, 1 mM sodium pyruvate and 2 mM L-glutamine and transfected using lipofectamine 2000 (all Invitrogen, Karlsruhe, Germany) according to the protocol provided by the manufacturer.

Electron microscopy

Transiently transfected PC12 cells were processed for immunogold electron microscopy essentially as described previously (29, 30). Briefly, cells were fixed in 8% formaldehyde 0.1% glutaraldehyde, dehydrated in graded ethanol series, followed by LR Gold embedding and UV-polymerization at –35°C. Ultrathin sections were incubated with primary ABs (pAB against reggie-1, mAB against EGFP). Visualization of reggie-1 was by protein A-gold (10-nm diameter) and goat anti-mouse $F(ab')_2$-gold (6 nm) for GFP, respectively.

FRAP experiments

Transiently transfected cells were viewed on poly-L-lysine-coated coverslips mounted in an Attofluor chamber (Invitrogen) using DMEM without phenol red supplemented with 5% FCS and 25 mM HEPES. FRAP experiments were carried out on a LSM 510 (Carl Zeiss, Jena, Germany) using a 63× Plan-Apochromat objective (na=1.4) with the room temperature stably set to 30°C. Transiently transfected cells expressing intermediate levels of R1FL-EGFP were chosen for FRAP analysis, allowing the use of similar microscope settings for all experiments. Images covering the whole cell were acquired in 12-bit mode at a rate of 2.5 frames/s. After acquiring a baseline of 30 frames using 1% transmission, a circular ROI of 1.3 μm in diameter was bleached at 100% transmission (10 repetitions, 100% laser power (15 mW)) and fluorescence recovery was observed for another 120 frames at 1% transmission. For analysis, the mean fluorescence of the bleached ROI and several control ROIs were plotted against time using the LSM 510 software (Carl Zeiss) and Sigma Plot (SPSS, Chicago, IL). The mobile fraction was calculated according to $M_F = (F_\infty–F_0)/(F_i–F_0)$ where F_∞ is the average fluorescence after full recovery, F_0 is the fluorescence immediately after the bleach and F_i is the average fluorescence before bleaching (34). The half-time of recovery $t_{1/2}$ was calculated by fitting the recovery curve to the empirical equation $F(t) = F_0 + ((F_\infty–F_0)*t)/(t + t_{1/2})$ (35, 36).

Superantigen-induced immunological synapse formation

Superantigen-induced immunological synapse formation using *staphylococcal* enterotoxin E (SEE) was essentially carried out as described (37, 38) with minor modifications. Briefly, Raji B lymphocytes were incubated with 5 μM CMAC cell tracker blue (Molecular Probes) in serum-free RPMI 1640 for 30 min at 37°C. Cells were washed and incubated with 2 μM SEE for 30 min at 37°C, washed again, and pelleted. An equal amount of Jurkat T cells was added to the Raji pellets, thoroughly mixed, and gently centrifuged to form a loose pellet. These pellets were incubated at 37°C for 30 min, then gently resuspended, and cells were allowed to settle on poly-L-lysine-coated coverslips for 30 min at 37°C. Cells were then fixed in paraformaldehyde and processed for immunofluorescence as described below.

Immunocytochemistry and confocal microscopy

Cells were stimulated as indicated, and immunocytochemistry was carried out as described previously (30, 31). Images were acquired using the LSM 510. Images of SEE-induced immunological synapses were acquired on an Axiovert 200M equipped with a Axiocam MR operated at full resolution (1388×1040 pixels) in 12-bit mode using a ×100 objective (na=1.3) and structured illumination using the Apotome system (all Carl Zeiss). Images were processed using the LSM 510 software or Axiovision 4.3 (Carl Zeiss).

ConA-induced cell spreading

Chambered coverslips (VWR, Darmstadt, Germany) were incubated with 10 μg/ml poly-D-lysine (30–70 kDa) for 15 min at room temperature, washed with PBS, incubated with 100 μg/ml Concanavalin A for 2 h and washed with PBS. Transiently transfected Jurkat T cells were allowed to spread on the ConA-coated coverslips for the indicated times at 37°C. Spreading was observed by confocal interference reflection microscopy (IRM) on a LSM 510 (Carl Zeiss) using

the 63× Plan-Apochromat objective, the 633-nm laser line, a HFT633 beamsplitter and no emission filter. For quantification of the IRM footprint area, the LSM 510 software was used.

Single cell Ca^{2+} imaging during spreading

Jurkat T cells transiently transfected with DsRed or DsRed-R1EA were sorted using a FACS Vantage SE (BD Biosciences, Erembodegem, Belgium), yielding a pure population of vital DsRed-expressing cells. For Ca^{2+} imaging, cells were loaded with 1 μM Fluo4-AM essentially as described previously for Fura2-AM (39), but loading was performed at 30°C to reduce compartmentalization of the dye. Cells were injected into chambered coverslips coated with ConA, as described above, and Ca^{2+} imaging was performed using a ×40 Plan-Neofluar objective (na=1.3) (Carl Zeiss) on the Axiovert 200M, with a frame rate of 30 frames/min. Tracings were normalized by calculating the ratio F/F0 (with F0 being the fluorescence before contact with the coverslip) and aligned according to the time point of contact with the coverslip.

Stimulated cell lysates and coimmunoprecipitation

Stimulated cell lysates were prepared as described previously (30). For coimmunoprecipitation, lysates were incubated first with the indicated antibodies and then with PBS-washed protein A-sepharose (Amersham, Uppsala, Sweden). Beads were collected by centrifugation, thoroughly washed with lysis buffer, and bound proteins eluted by boiling in 2× Laemmli sample buffer. SDS-PAGE and Western blotting was performed according to standard procedures.

RESULTS

Membrane localization and lateral mobility of reggie-1-EGFP in PC12 cells

To characterize the behavior of reggie-1 in T cell caps as opposed to the membrane outside this structure, we determined the lateral mobility of reggie-1 in PC12 and Jurkat T cells using FRAP. To ensure a correct plasma membrane localization of reggie-1-EGFP (R1FL-EGFP), we performed immunogold labeling and electron microscopy of transiently transfected PC12 cells. Endogenous reggie-1 was found in microdomains of a typical size of ≤0.1 μm (Fig. 1*A*) as reported previously for various other cell lines (29, 30). In cells transiently transfected with R1FL-EGFP, the double gold labeling strictly coincided, showing colocalization of reggie-1 and the fusion protein, thus suggesting that R1FL-EGFP is correctly incorporated in reggie microdomains (Fig. 1*A*).

FRAP experiments demonstrated high lateral mobility of R1FL-EGFP at the plasma membrane of PC12 cells. The fluorescence derived from R1FL-EGFP in the bleached region recovered with a half time of $t_{1/2}$=3.9 ± 2 s (n=19, ±SD). A mobile fraction of M_F=0.8 (±0.1, ±SD) suggested almost unrestricted lateral diffusion (Fig. 1*B*). Interestingly, at the basis of membrane protrusions, the lateral diffusion of reggie-1 was significantly reduced (M_F=0.61±0.13, n=18, ±SD, P<0.01 (Student's t test)).

Stabilization of reggie-1 in preformed caps in Jurkat T cells

Because reggie-1 is organized in preformed caps in T cells, we performed similar FRAP experiments in Jurkat T lymphocytes. R1FL-EGFP accumulated in ~50–60% of the transfected

cells in a preformed cap. Bleaching a spot within the preformed cap, almost no recovery of fluorescence was observed. A mobile fraction of only M_F = 0.12 (±0.09, *n*=12, ±SD) indicated nearly complete immobilization of reggie-1 in the region of the preformed cap (Fig. 2*B*, *C*). By contrast, if the bleach spot was placed outside of the preformed cap or in cells that did not show any localized accumulation of reggie-1, a fast and almost complete recovery occurred with a half time of $t_{1/2}$ = 1.5 ± 0.5 s (*n*=15, ±SD) and a mobile fraction of M_F = 0.72 ± 0.12 (±SD) (Fig. 2*A*, *C*), similar to PC12 cells. This indicates that reggie-1 is selectively immobilized in the region of the preformed cap, whereas it remains highly mobile at the plasma membrane outside of the caps.

Next, we investigated the mechanism of reggie-1 stabilization in the preformed cap. Treatment with methyl-β-cyclodextrin (MβCD) is known to disrupt lipid microdomains by cholesterol depletion. The occurrence of preformed reggie caps was not affected by MβCD treatment, as reported previously (31). Also, the immobilization of R1FL-EGFP in these caps was unaffected by MβCD treatment (data not shown). Thus, the remarkable stabilization of reggie-1 in preformed caps is not simply the result of lipid raft clustering but must involve other mechanisms such as stabilization by cytoskeletal elements. Indeed, when the actin cytoskeleton was disrupted by latrunculin A (data not shown) or cytochalasin D, the cells lost their preformed caps, and reggie-1 was evenly distributed all along the plasma membrane (Fig. 2*D*).

Recruitment of signaling molecules to stable reggie caps during T cell activation

We have previously shown that signaling induced by cross-linking of lipid rafts by cholera toxin or antibody-mediated cross-linking of the GPI-anchored cellular prion protein PrP^c elicits the accumulation of signaling molecules in the region of the preformed reggie cap (29–31). Likewise, activation of the cell by cross-linking of cell surface proteins using the mitogenic lectin ConA resulted in the accumulation of for example, LAT and the Src-family kinase lck in the cap region, while both proteins were evenly distributed along the plasma membrane in resting cells (Fig. 3*A*). TCR signaling is a highly dynamic process in which signaling molecules rapidly move between the TCR signaling complex and other compartments (19). Thus, we next investigated whether the stabilization of reggie-1 persists in stimulated cells. Activation of the cell by ConA coupled to the fluorophore Alexa 568 resulted in an accumulation of ConA-fluorescence in the region of the reggie cap (Fig. 3*B*, inset). Measuring the mobility of R1FL-EGFP in "stimulated caps" in FRAP experiments revealed a mobile fraction of M_F = 0.09 ± 0.09 (*n*=15; ±SD), indicating complete immobilization of reggie-1 (Fig. 3*B*). These data demonstrate that the preformed reggie caps are stable platforms before, as well as during, stimulation of the cell.

Several bacterial toxins can act as superantigens leading to a specific interaction of MHC with the TCR complex (40). *Staphylococcus* enterotoxin E (SEE) presented by Raji B cells is known to induce a strong proliferative response in Jurkat T cells (41). To explore the physiological significance of reggie caps, we investigated the localization of reggie-1 in the immunological synapse of Jurkat T cells and SEE-bearing Raji B cell conjugates. In the absence of superantigen, Jurkat T and Raji B cells were seldom associated and in cell-cell contacts neither reggie-1 nor LAT accumulated at the interphase (Fig. 3*C*). By contrast, in the presence of SEE, numerous intimate and stable conjugates between Raji B and Jurkat T cells were formed. In addition, LAT

and reggie-1 were recruited to the synapse (Fig. 3*C*), confirming the physiological significance of reggie-based signaling platforms for T cell signaling.

The C terminus of reggie-1 is essential for its incorporation into the preformed cap

To define the structural requirements of reggie-1 to incorporate into preformed caps, we generated a variety of deletion mutants (Fig. 4*A*). R1FL-EGFP clearly colocalized with endogenous reggie-2 in preformed caps, as expected (Fig. 4*B*). By contrast, the R1L1 mutant lacking the C-terminal part of reggie-1, including the EA repeat region, which was predicted to form coiled coils (25, 42), localized to the plasma membrane but failed to accumulate in the preformed cap demarcated by endogenous reggie-2 (Fig. 4*C*). The C terminus of reggie-1 was shown to be essential and sufficient for the formation of reggie-1 oligomers (26), which we verified using biochemical cross-linking experiments (G. Solis and C.A.O. Stuermer, unpublished results).

A trans-negative reggie-1 mutant inhibits macrodomain assembly after T cell stimulation

On the basis of these insights, we generated a N-terminal deletion mutant of reggie-1 consisting only of the C-terminal, EA-rich domain (R1EA, Fig. 4*A*). R1EA was still able to oligomerize with the full-length reggies (G. Solis and C.A.O. Stuermer, unpublished data). To test whether R1EA interferes with the oligomerization of the endogenous reggies, we expressed DsRed-R1EA with R1FL-EGFP in Jurkat T cells. Strikingly, the expression of DsRed-R1EA significantly reduced the accumulation of R1FL-EGFP in preformed caps compared with cells coexpressing R1FL-EGFP and pDsRed as control (Fig. 5*A*).

More importantly, expression of EGFP-R1EA interfered with raft polarization and clustering after stimulation. Cross-linking of the plasma membrane ganglioside GM1 by cholera toxin (CTX) leads to the accumulation of clustered rafts in the cap region and thereby induces signaling (4, 21, 31). CTX-cross-linking induced GM1 capping in the majority of control cells transiently transfected with pEGFP (Fig. 5*B*). Expression of EGFP-R1EA significantly reduced the number of cells bearing a GM1 cap after CTX cross-linking. In most EGFP-R1EA expressing cells, GM1/CTX staining was strongly patched, but these patches did not coalesce to form a macrodomain in the cap (Fig. 5*B*). Similarly, expression of EGFP-R1EA strongly reduced macrodomain assembly and capping after ConA stimulation. In EGFP-R1EA expressing cells, ConA fluorescence was again patchy, with clusters distributed around the cell (Fig. 5*C*). Hence, the loss of preformed reggie caps by expressing a trans-negative deletion mutant significantly reduced the efficiency of raft polarization and macrodomain assembly after T cell stimulation.

Trans-negative reggie-1 mutant impairs stimulation-induced T cell spreading

To substantiate the role of preformed reggie caps in T cell signaling, we investigated stimulation-induced T cell spreading. Toward this end, coverslips were coated with ConA as a polarizing stimulus, requiring responding cells to undergo massive morphological changes in order to maximize contact with the stimulatory surface (43). This spreading response can be monitored by interference reflection microscopy (IRM), where contrast is generated by interference of light reflected at cellular membranes contacting the coverslip with light reflected at the glass-water interface. Cells adhering to the coverslip therefore appear dark (44).

Only weak adhesion and no spreading of T cells was observed on coverslips coated with poly-L-lysine alone or in combination with BSA (data not shown). However, untransfected T cells or cells transiently transfected with the control vector pEGFP spread out completely on ConA coated coverslips within 10 min. First contacts were made by thin filopodia, followed by highly mobile membrane protrusions; finally, the cells flattened completely (Fig. 5*D*). The cells exhibited a round regular footprint, often with thin filopodia at the periphery (Fig. 5*D*, *F*). Although the cells did not spread any further, we observed constant dynamic remodeling of the cell-substrate contacts in the periphery. Jurkat T cells transiently transfected with EGFP-R1EA failed to undergo complete spreading, although they still adhered to ConA-coated coverslips. The spreading response was slower, and spreading ended before a regular round footprint was established (Fig. 5*E*). Moreover, we often observed long and irregularly organized filopodia at the periphery of EGFP-R1EA expressing cells (Fig. 5*E*, *F*). To substantiate these morphological differences, we quantified the footprint area observed by IRM in pEGFP- and EGFP-R1EA transfected cells after 15 min of spreading. The footprint area of EGFP-R1EA-transfected cells was significantly smaller ($P<0.01$ (Student's t test)), covering an area of only 550 μm^2 ($\pm$170 μm^2, $n=103\pm$SD) vs. an average footprint area of 760 μm^2 ($\pm$225 μm^2, $n=119\pm$SD) in pEGFP control cells.

Reggie-1 regulates Vav localization

To elucidate which intracellular signaling pathways depend on reggie-1, we optimized transfection conditions for Jurkat T cells resulting in an transfection efficiency of >50%, permitting biochemical analysis of signaling components using phospho-specific antibodies. The expression of R1EA did neither significantly affect the activation of the TCR proximal tyrosine kinase ZAP-70, nor of the downstream effector MAP kinase ERK1/2 after ConA stimulation, although tyrosine phosphorylation of ZAP-70 was slightly diminished in R1EA-expressing cells (Fig. 6*A*). Ca^{2+} signaling during spreading on ConA-coated coverslips was indistinguishable in DsRed-R1EA- and control-transfected cells, as assessed by single cell Ca^{2+} imaging using Fluo4. Neither the mean response nor the behavior of the individual cells changed significantly by R1EA expression (Fig. 6*B*). These results suggest that interfering with reggie-1 function does not impair general signaling efficiency but rather affects signaling events controlling cytoskeletal dynamics because both macrodomain assembly and cell spreading are dependent on cytoskeletal remodeling.

The guanine nucleotide exchange factor Vav is a key regulator of the actin cytoskeleton by controlling the activity of Rho-family GTPases (45, 46). Therefore, we investigated on an interaction of reggie-1 with Vav. Indeed, reggie-1 and Vav coclustered at the plasma membrane upon spreading in ConA-coated coverslips (Fig. 6*C*). To formally prove an interaction between these proteins, we performed coimmunoprecipitation experiments of endogenous Vav and reggie-1. Immunoprecipitation of Vav reliably coprecipitated reggie-1 in resting (Fig. 6*D*) and stimulated cells (data not shown), suggesting that both proteins are part of a multiprotein complex in T cells.

Interfering with reggie function by expressing R1EA severely disturbed the proper positioning of Vav. In mock-transfected cells, spreading on ConA-coated coverslips induced the formation of Vav-containing clusters on the entire footprint area of an activated cell (Fig. 6*E*). By contrast, R1EA-expression provoked a mislocalization of Vav, where Vav clusters were concentrated in

the region of the initial contact but were virtually absent in the periphery (Fig. 6*E*). Thus interfering with reggie function leads to an aberrant localization of Vav clusters, resulting in defects in cytoskeletal remodeling.

DISCUSSION

Our results show for the first time a functional contribution of the preformed reggie caps in T cell signaling. The preformed reggie caps are remarkably stable structures. A trans-negative reggie-1 mutant, which blocked the accumulation of the reggies in a preformed cap, inhibited raft polarization and macrodomain assembly after stimulation with ConA or by CTX cross-linking. Moreover, the localization of Vav and hence cytoskeletal rearrangements during ConA-induced cell spreading were severely disturbed, whereas the activation of the MAP kinases ERK1/2 and Ca^{2+} signaling were not affected. Thus, the preexisting priming platforms provided by the reggies function as coordinating scaffolds for stimulation-induced cytoskeletal remodeling.

The preformed reggie caps impose polarity on lymphocytes, both in stable cells lines and in primary T cells (30, 31). Our FRAP analysis showed that the preformed reggie caps are remarkably stable before and during cell stimulation. This stabilization was independent of the cholesterol content of the membrane but dependent on the integrity of the actin cytoskeleton. Whether reggie clusters are directly linked to the actin cytoskeleton or whether the preformed cap is surrounded by a diffusion barrier anchored to the actin cytoskeleton remains to be clarified. However, we have preliminary evidence for an interaction of reggie-1 with actin (M.F. Langhorst, G. Solis, E. Rivera-Milla and C.A.O. Stuermer, unpublished observations), suggesting that the reggie clusters at the plasma membrane might be anchored by binding of the reggies to the cortical actin cytoskeleton.

In stimulated cells, key signaling molecules translocate to the preformed reggie caps. This translocation is considered to depend on lipid raft clustering (3, 29–31) in the region of the preformed reggie caps. This is further supported by reports showing an increased biochemical association of LAT, lck, IKKβ, and vimentin with reggie complexes after CD3/CD28 costimulation (32, 33). Our results directly demonstrate the functional importance of the preformed reggie caps: The trans-negative reggie-1 mutant R1EA inhibited preformed cap assembly and the clustering of rafts after stimulation of the cell, which suggests a role of the preformed reggie caps in coordinating raft polarization and macrodomain formation during T cell activation.

Recent reports challenged the importance of lipid rafts in T cell activation. Douglass and Vale recently reported the formation of microdomains during T cell activation based solely on protein–protein-interactions (47). In this study, cells were activated solely by anti-CD3 antibodies, while other studies have shown that costimulation by CD28 is necessary to induce extensive raft clustering (22). Furthermore, the different experimental approaches used in different studies result in different definitions of lipid rafts (reviewed in Ref. 11). He et al. proposed in a recent review, that of the many different microdomains present in a cell, only a specific subset of rafts is involved in the dynamic assembly of the stable macrodomain surrounding engaged TCRs (12). Such an ordered macrodomain at the site of lymphocyte activation was recently directly visualized using the order-sensitive, fluorescent dye Laurdan

(18), confirming earlier observations that T cell activation triggers the assembly of a raft-like stable macrodomain, whereas rafts may be small and highly dynamic in resting cells.

Macrodomain assembly in T cells was shown to be regulated by actin cytoskeleton remodeling (18, 20, 45, 48, 49). The spreading response of T cells on stimulatory surfaces represents a simplified assay for stimulation-induced morphological changes and cytoskeletal rearrangements and is often used to evaluate the effects of a given protein on stimulation-induced actin remodeling (43, 50). Our observation that the trans-negative reggie-1 mutant severely impaired T cell spreading further supports a functional role of the reggie platforms in T cell signaling and hints to a role in the regulation of actin dynamics. Both the inhibition of macrodomain assembly and the impairment of the spreading response by the trans-negative reggie mutant can be explained by the association of reggie-1 with the guanine exchange factor Vav. Vav is a key regulator of the cytoskeleton in T cells (45, 46) but may also influence directly or indirectly other signaling pathways (51, 52). Vav was shown to be essential for raft clustering in T cells. In Vav-deficient T cells, rafts did not translocate to the immunological synapse and, most interestingly, dominant-negative Vav mutants inhibited raft polarization and clustering in T cells after CTX cross-linking (21). This is indeed surprisingly similar to the effects of the trans-negative reggie-1 mutant observed in our present study. Furthermore, Vav function is regulated by fyn and lck (53, 54), which provides another link to the reggies, as both Src family kinases are associated with the reggies (29, 30, 55). Upon expression of the trans-negative reggie mutant R1EA, we observed an incorrect positioning of Vav in cells spreading on a stimulatory surface, resulting in aberrant and incomplete spreading, suggesting that reggie-1 regulates the localization of Vav. Interestingly, an impairment of the spreading response similar to our results was observed in Jurkat T cells lacking the adaptor protein LAT (43). LAT is associated with reggie complexes, and this association increases upon stimulation (32, 33). Via its interaction with SLP-76, LAT is also involved in the activation of Vav (56). Thus, reggie-associated protein complexes, including e.g., Vav, lck, fyn, and LAT, are probably involved in controlling stimulation-induced actin remodeling in T cells.

Indeed, several reports implicated the reggies in the regulation of actin dynamics in various other cell types. Overexpression of reggie-1 induces filopodia formation in some cell types (26, 57). Reggie-2 binds to the SoHo domain of the adaptor proteins of the vinexin family (58), which, in turn, bind to signaling molecules like the adaptor protein c-Cbl, the tyrosine kinase c-Abl and regulators of the cytoskeleton like vinculin, Sos and Grb4 via their C-terminal SH3 domains (59). The assembly of such a multiprotein complex was shown to be essential for Glut4 trafficking in adipocytes (55, 60) and for neuritogenesis in differentiating PC12 cells (61). Our observation that reggie-1 forms stabilized structures at the basis of membrane protrusions in PC 12 cells also agrees with our model, in which reggie clusters provide a scaffold for protein complex assembly regulating cytoskeletal dynamics.

Reggie proteins define specialized plasma membrane microdomains, in which reggie oligomers provide a scaffold for multiprotein complex assembly, similar to, but distinct from, caveolae (reviewed in Ref. 28). In T cells the reggies apparently provide preexisting priming platforms upon which multiprotein complexes assemble after stimulation to coordinate cytoskeletal remodeling. As some of these key regulators of the actin cytoskeleton are already associated with the reggies in resting cells, one can imagine a feed-forward mechanism where few protein complexes already assembled on the reggie scaffolds initiate the signaling events necessary for

raft polarization and macrodomain assembly, which then leads to the accumulation and activation of more signaling complexes in the cap. Without the preformed reggie cap, spatial information important for macrodomain assembly is apparently missing. Although raft clustering still occurs, these small clusters do not coalesce to form a macrodomain in the cap. Therefore, the reggies appear to be an important factor in the regulation of actin dynamics during T cell activation.

ACKNOWLEDGMENTS

We thank Ms. L. Nejedli and S. Kolassa for preparing EM samples and Ralf Fliegert for helpful comments on the manuscript. This work was supported by grants from the Deutsche Forschungsgemeinschaft DFG (SFB-TR11), the Ministerium Forschung, Wissenschaft und Kunst Baden-Württemberg (TSE program) and the Fonds der Chemischen Industrie.

REFERENCES

1. Golub, T., Wacha, S., and Caroni, P. (2004) Spatial and temporal control of signaling through lipid rafts. *Curr. Opin. Neurobiol.* **14,** 542–550

2. Brown, D. A., and London, E. (1998) Functions of lipid rafts in biological membranes. *Annu. Rev. Cell Dev. Biol.* **14,** 111–136

3. Simons, K., and Toomre, D. (2000) Lipid rafts and signal transduction. *Nat. Rev. Mol. Cell Biol.* **1,** 31–39

4. Janes, P. W., Ley, S. C., and Magee, A. I. (1999) Aggregation of lipid rafts accompanies signaling via the T cell antigen receptor. *J. Cell Biol.* **147,** 447–461

5. Dykstra, M., Cherukuri, A., Sohn, H. W., Tzeng, S. J., and Pierce, S. K. (2003) Location is everything: lipid rafts and immune cell signaling. *Annu. Rev. Immunol.* **21,** 457–481

6. Zhang, W., Trible, R. P., and Samelson, L. E. (1998) LAT palmitoylation: its essential role in membrane microdomain targeting and tyrosine phosphorylation during T cell activation. *Immunity* **9,** 239–246

7. Kabouridis, P. S., Magee, A. I., and Ley, S. C. (1997) S-acylation of LCK protein tyrosine kinase is essential for its signalling function in T lymphocytes. *EMBO J.* **16,** 4983–4998

8. Filipp, D., Leung, B. L., Zhang, J., Veillette, A., and Julius, M. (2004) Enrichment of lck in lipid rafts regulates colocalized fyn activation and the initiation of proximal signals through TCR alpha beta. *J. Immunol.* **172,** 4266–4274

9. Fragoso, R., Ren, D., Zhang, X., Su, M. W., Burakoff, S. J., and Jin, Y. J. (2003) Lipid raft distribution of CD4 depends on its palmitoylation and association with Lck, and evidence for CD4-induced lipid raft aggregation as an additional mechanism to enhance CD3 signaling. *J. Immunol.* **170,** 913–921

10. Munro, S. (2003) Lipid rafts: elusive or illusive? *Cell* **115,** 377–388

11. Lichtenberg, D., Goni, F. M., and Heerklotz, H. (2005) Detergent-resistant membranes should not be identified with membrane rafts. *Trends Biochem. Sci.* **30,** 430–436

12. He, H. T., Lellouch, A., and Marguet, D. (2005) Lipid rafts and the initiation of T cell receptor signaling. *Semin. Immunol.* **17,** 23–33

13. Sharma, P., Varma, R., Sarasij, R. C., Ira, Gousset, K., Krishnamoorthy, G., Rao, M., and Mayor, S. (2004) Nanoscale organization of multiple GPI-anchored proteins in living cell membranes. *Cell* **116**, 577–589

14. Subczynski, W. K., and Kusumi, A. (2003) Dynamics of raft molecules in the cell and artificial membranes: approaches by pulse EPR spin labeling and single molecule optical microscopy. *Biochim. Biophys. Acta* **1610,** 231–243

15. Gomez-Mouton, C., Abad, J. L., Mira, E., Lacalle, R. A., Gallardo, E., Jimenez-Baranda, S., Illa, I., Bernad, A., Manes, S., and Martinez, A. C. (2001) Segregation of leading-edge and uropod components into specific lipid rafts during T cell polarization. *Proc. Natl. Acad. Sci. USA* **98,** 9642–9647

16. Valensin, S., Paccani, S. R., Ulivieri, C., Mercati, D., Pacini, S., Patrussi, L., Hirst, T., Lupetti, P., and Baldari, C. T. (2002) F-actin dynamics control segregation of the TCR signaling cascade to clustered lipid rafts. *Eur. J. Immunol.* **32,** 435–446

17. Rodgers, W., Farris, D., and Mishra, S. (2005) Merging complexes: properties of membrane raft assembly during lymphocyte signaling. *Trends Immunol.* **26,** 97–103

18. Gaus, K., Chklovskaia, E., Fazekas de St Groth, B., Jessup, W., and Harder, T. (2005) Condensation of the plasma membrane at the site of T lymphocyte activation. *J. Cell Biol.* **171,** 121–131

19. Gordy, C., Mishra, S., and Rodgers, W. (2004) Visualization of antigen presentation by actin-mediated targeting of glycolipid-enriched membrane domains to the immune synapse of B cell APCs. *J. Immunol.* **172,** 2030–2038

20. Rodgers, W., and Zavzavadjian, J. (2001) Glycolipid-enriched membrane domains are assembled into membrane patches by associating with the actin cytoskeleton. *Exp. Cell Res.* **267,** 173–183

21. Villalba, M., Bi, K., Rodriguez, F., Tanaka, Y., Schoenberger, S., and Altman, A. (2001) Vav1/Rac-dependent actin cytoskeleton reorganization is required for lipid raft clustering in T cells. *J. Cell Biol.* **155,** 331–338

22. Viola, A., Schroeder, S., Sakakibara, Y., and Lanzavecchia, A. (1999) T lymphocyte costimulation mediated by reorganization of membrane microdomains. *Science* **283,** 680–682

23. Schulte, T., Paschke, K. A., Laessing, U., Lottspeich, F., and Stuermer, C. A. (1997) Reggie-1 and reggie-2, two cell surface proteins expressed by retinal ganglion cells during axon regeneration. *Development* **124,** 577–587

24. Lang, D. M., Lommel, S., Jung, M., Ankerhold, R., Petrausch, B., Laessing, U., Wiechers, M. F., Plattner, H., and Stuermer, C. A. (1998) Identification of reggie-1 and reggie-2 as plasma membrane-associated proteins which cocluster with activated GPI-anchored cell adhesion molecules in non-caveolar micropatches in neurons. *J. Neurobiol.* **37,** 502–523

25. Bickel, P. E., Scherer, P. E., Schnitzer, J. E., Oh, P., Lisanti, M. P., and Lodish, H. F. (1997) Flotillin and epidermal surface antigen define a new family of caveolae-associated integral membrane proteins. *J. Biol. Chem.* **272,** 13,793–13,802

26. Neumann-Giesen, C., Falkenbach, B., Beicht, P., Claasen, S., Luers, G., Stuermer, C. A., Herzog, V., and Tikkanen, R. (2004) Membrane and raft association of reggie-1/flotillin-2: role of myristoylation, palmitoylation and oligomerization and induction of filopodia by overexpression. *Biochem. J.* **378,** 509–518

27. Morrow, I. C., Rea, S., Martin, S., Prior, I. A., Prohaska, R., Hancock, J. F., James, D. E., and Parton, R. G. (2002) Flotillin-1/reggie-2 traffics to surface raft domains via a novel golgi-independent pathway. Identification of a novel membrane targeting domain and a role for palmitoylation. *J. Biol. Chem.* **277,** 48,834–48,841

28. Langhorst, M. F., Reuter, A., and Stuermer, C. A. (2005) Scaffolding microdomains and beyond: the function of reggie/flotillin proteins. *Cell. Mol. Life Sci.* **62,** 2228–2240

29. Stuermer, C. A., Lang, D. M., Kirsch, F., Wiechers, M., Deininger, S. O., and Plattner, H. (2001) Glycosylphosphatidyl inositol-anchored proteins and fyn kinase assemble in noncaveolar plasma membrane microdomains defined by reggie-1 and -2. *Mol. Biol. Cell* **12,** 3031–3045

30. Stuermer, C. A., Langhorst, M. F., Wiechers, M. F., Legler, D. F., Hannbeck von Hanwehr, S., Guse, A. H., and Plattner, H. (2004) PrPc capping in T cells promotes its association with the lipid raft proteins reggie-1 and reggie-2 and leads to signal transduction. *FASEB J.* express article 10.1096/fj.04-2150fje

31. Rajendran, L., Masilamani, M., Solomon, S., Tikkanen, R., Stuermer, C. A., Plattner, H., and Illges, H. (2003) Asymmetric localization of flotillins/reggies in preassembled platforms confers inherent polarity to hematopoietic cells. *Proc. Natl. Acad. Sci. USA* **100,** 8241–8246

32. Slaughter, N., Laux, I., Tu, X., Whitelegge, J., Zhu, X., Effros, R., Bickel, P., and Nel, A. (2003) The flotillins are integral membrane proteins in lipid rafts that contain TCR-associated signaling components: implications for T-cell activation. *Clin. Immunol.* **108,** 138–151

33. Tu, X., Huang, A., Bae, D., Slaughter, N., Whitelegge, J., Crother, T., Bickel, P. E., and Nel, A. (2004) Proteome analysis of lipid rafts in Jurkat cells characterizes a raft subset that is involved in NF-κB activation. *J. Proteome Res.* **3,** 445–454

34. Reits, E. A., and Neefjes, J. J. (2001) From fixed to FRAP: measuring protein mobility and activity in living cells. *Nat. Cell Biol.* **3,** E145–E147

35. Kwon, G., Axelrod, D., and Neubig, R. R. (1994) Lateral mobility of tetramethylrhodamine (TMR) labelled G protein alpha and beta gamma subunits in NG 108-15 cells. *Cell. Signal.* **6,** 663–679

36. Klonis, N., Rug, M., Harper, I., Wickham, M., Cowman, A., and Tilley, L. (2002) Fluorescence photobleaching analysis for the study of cellular dynamics. *Eur. Biophys. J.* **31,** 36–51

37. Mittelbrunn, M., Yanez-Mo, M., Sancho, D., Ursa, A., and Sanchez-Madrid, F. (2002) Cutting edge: dynamic redistribution of tetraspanin CD81 at the central zone of the immune synapse in both T lymphocytes and APC. *J. Immunol.* **169,** 6691–6695

38. Morgan, M. M., Labno, C. M., Van Seventer, G. A., Denny, M. F., Straus, D. B., and Burkhardt, J. K. (2001) Superantigen-induced T cell:B cell conjugation is mediated by LFA-1 and requires signaling through Lck, but not ZAP-70. *J. Immunol.* **167,** 5708–5718

39. Langhorst, M. F., Schwarzmann, N., and Guse, A. H. (2004) Ca^{2+} release via ryanodine receptors and Ca^{2+} entry: major mechanisms in NAADP-mediated Ca^{2+} signaling in T-lymphocytes. *Cell. Signal.* **16,** 1283–1289

40. Petersson, K., Forsberg, G., and Walse, B. (2004) Interplay between superantigens and immunoreceptors. *Scand. J. Immunol.* **59,** 345–355

41. Herman, A., Croteau, G., Sekaly, R. P., Kappler, J., and Marrack, P. (1990) HLA-DR alleles differ in their ability to present staphylococcal enterotoxins to T cells. *J. Exp. Med.* **172,** 709–717

42. Schroeder, W. T., Stewart-Galetka, S., Mandavilli, S., Parry, D. A., Goldsmith, L., and Duvic, M. (1994) Cloning and characterization of a novel epidermal cell surface antigen (ESA). *J. Biol. Chem.* **269,** 19,983–19,991

43. Bunnell, S. C., Kapoor, V., Trible, R. P., Zhang, W., and Samelson, L. E. (2001) Dynamic actin polymerization drives T cell receptor-induced spreading: a role for the signal transduction adaptor LAT. *Immunity* **14,** 315–329

44. Weber, I. (2003) Reflection interference contrast microscopy. *Methods Enzymol.* **361,** 34–47

45. Holsinger, L. J., Graef, I. A., Swat, W., Chi, T., Bautista, D. M., Davidson, L., Lewis, R. S., Alt, F. W., and Crabtree, G. R. (1998) Defects in actin-cap formation in Vav-deficient mice implicate an actin requirement for lymphocyte signal transduction. *Curr. Biol.* **8,** 563–572

46. Fischer, K. D., Kong, Y. Y., Nishina, H., Tedford, K., Marengere, L. E., Kozieradzki, I., Sasaki, T., Starr, M., Chan, G., Gardener, S., et al. (1998) Vav is a regulator of cytoskeletal reorganization mediated by the T-cell receptor. *Curr. Biol.* **8,** 554–562

47. Douglass, A. D., and Vale, R. D. (2005) Single-molecule microscopy reveals plasma membrane microdomains created by protein-protein networks that exclude or trap signaling molecules in T cells. *Cell* **121,** 937–950

48. Harder, T., and Simons, K. (1999) Clusters of glycolipid and glycosylphosphatidylinositol-anchored proteins in lymphoid cells: accumulation of actin regulated by local tyrosine phosphorylation. *Eur. J. Immunol.* **29,** 556–562

49. Wulfing, C., and Davis, M. M. (1998) A receptor/cytoskeletal movement triggered by costimulation during T cell activation. *Science* **282,** 2266–2269

50. Barda-Saad, M., Braiman, A., Titerence, R., Bunnell, S. C., Barr, V. A., and Samelson, L. E. (2005) Dynamic molecular interactions linking the T cell antigen receptor to the actin cytoskeleton. *Nat. Immunol.* **6,** 80–89

51. Costello, P. S., Walters, A. E., Mee, P. J., Turner, M., Reynolds, L. F., Prisco, A., Sarner, N., Zamoyska, R., and Tybulewicz, V. L. (1999) The Rho-family GTP exchange factor Vav is a critical transducer of T cell receptor signals to the calcium, ERK, and NF-κB pathways. *Proc. Natl. Acad. Sci. USA* **96,** 3035–3040

52. Cao, Y., Janssen, E. M., Duncan, A. W., Altman, A., Billadeau, D. D., and Abraham, R. T. (2002) Pleiotropic defects in TCR signaling in a Vav-1-null Jurkat T-cell line. *EMBO J.* **21,** 4809–4819

53. Huang, J., Tilly, D., Altman, A., Sugie, K., and Grey, H. M. (2000) T-cell receptor antagonists induce Vav phosphorylation by selective activation of Fyn kinase. *Proc. Natl. Acad. Sci. USA* **97,** 10,923–10,929

54. Han, J., Das, B., Wei, W., Van Aelst, L., Mosteller, R. D., Khosravi-Far, R., Westwick, J. K., Der, C. J., and Broek, D. (1997) Lck regulates Vav activation of members of the Rho family of GTPases. *Mol. Cell. Biol.* **17,** 1346–1353

55. Liu, J., Deyoung, S. M., Zhang, M., Dold, L. H., and Saltiel, A. R. (2005) The stomatin/prohibitin/flotillin/HflK/C domain of flotillin-1 contains distinct sequences that direct plasma membrane localization and protein interactions in 3T3-L1 adipocytes. *J. Biol. Chem.* **280,** 16,125–16,134

56. Samelson, L. E. (2002) Signal transduction mediated by the T cell antigen receptor: the role of adapter proteins. *Annu. Rev. Immunol.* **20,** 371–394

57. Hazarika, P., Dham, N., Patel, P., Cho, M., Weidner, D., Goldsmith, L., and Duvic, M. (1999) Flotillin 2 is distinct from epidermal surface antigen (ESA) and is associated with filopodia formation. *J. Cell. Biochem.* **75,** 147–159

58. Kimura, A., Baumann, C. A., Chiang, S. H., and Saltiel, A. R. (2001) The sorbin homology domain: a motif for the targeting of proteins to lipid rafts. *Proc. Natl. Acad. Sci. USA* **98,** 9098–9103

59. Kioka, N., Ueda, K., and Amachi, T. (2002) Vinexin, CAP/ponsin, ArgBP2: a novel adaptor protein family regulating cytoskeletal organization and signal transduction. *Cell Struct. Funct.* **27,** 1–7

60. Baumann, C. A., Ribon, V., Kanzaki, M., Thurmond, D. C., Mora, S., Shigematsu, S., Bickel, P. E., Pessin, J. E., and Saltiel, A. R. (2000) CAP defines a second signalling pathway required for insulin-stimulated glucose transport. *Nature* **407,** 202–207

61. Haglund, K., Ivankovic-Dikic, I., Shimokawa, N., Kruh, G. D., and Dikic, I. (2004) Recruitment of Pyk2 and Cbl to lipid rafts mediates signals important for actin reorganization in growing neurites. *J. Cell Sci.* **117,** 2557–2568

Received July 25, 2005; accepted December 5, 2005

Fig. 1

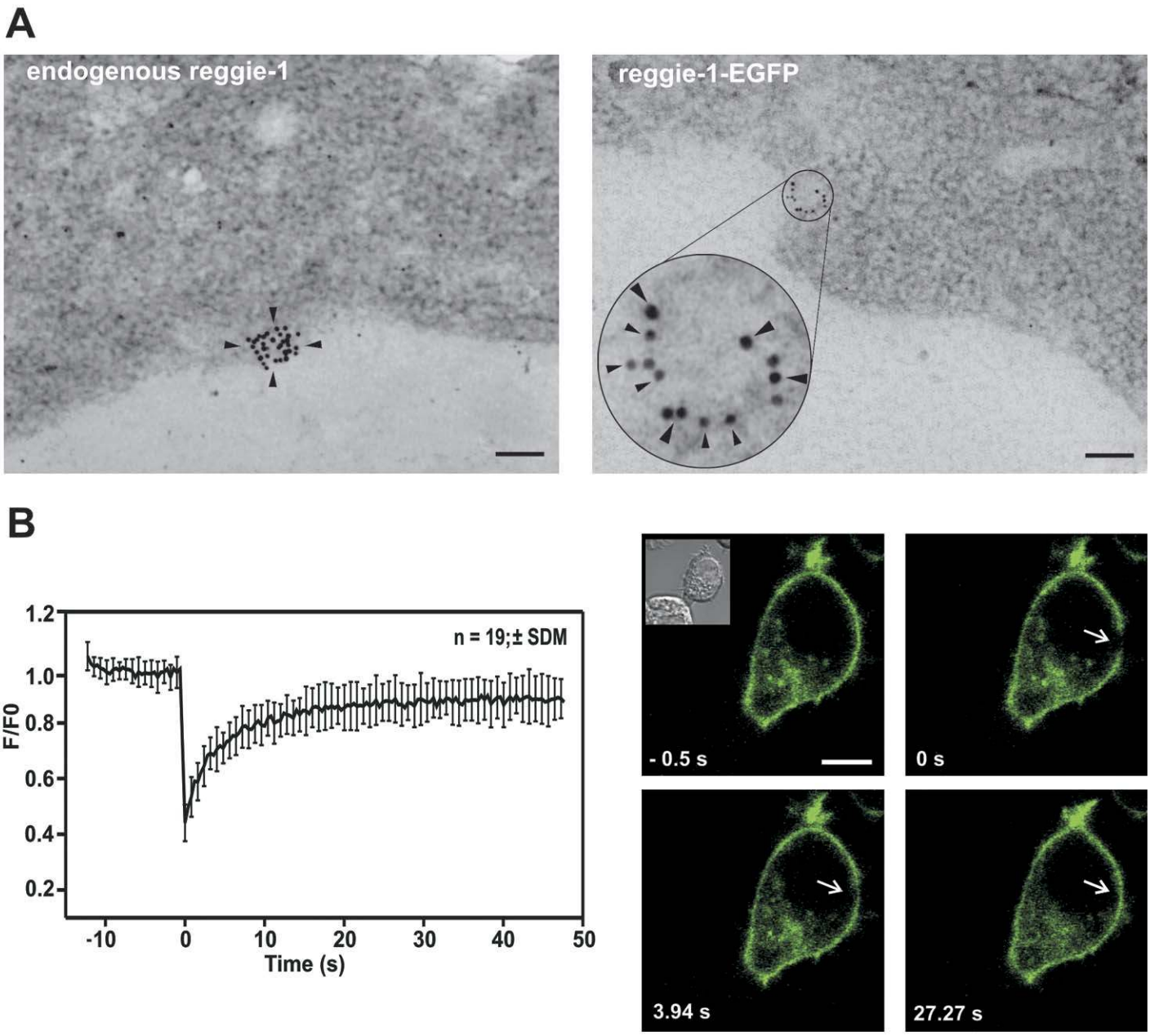

Figure 1. Reggie microdomains and analysis of the lateral mobility of reggie-1 in PC12 cells: ***A*)** Electron microscopy of immunogold staining on grazing sections of either wild-type PC12 or cells transiently transfected with R1FL-EGFP. Endogenous reggie-1 was visualized by 10-nm gold particles at the cell membrane (***left***). Colocalization of reggie-1 (10 nm gold, large arrowheads) and EGFP (6 nm gold, small arrowheads) at the cell membrane in a cell expressing R1FL-EGFP (***right***) (Scale bar = 0.1 μm) ***B*)** FRAP analysis of the lateral mobility of reggie-1 (R1FL-EGFP) at the plasma membrane of PC12 cells. Tracings from 19 cells from 5 independent experiments were averaged. Images of one representative cell at key time points are shown, the inset shows a DIC image of the same cell (arrows indicate the bleached region; scale bar = 5 μm)

Fig. 2

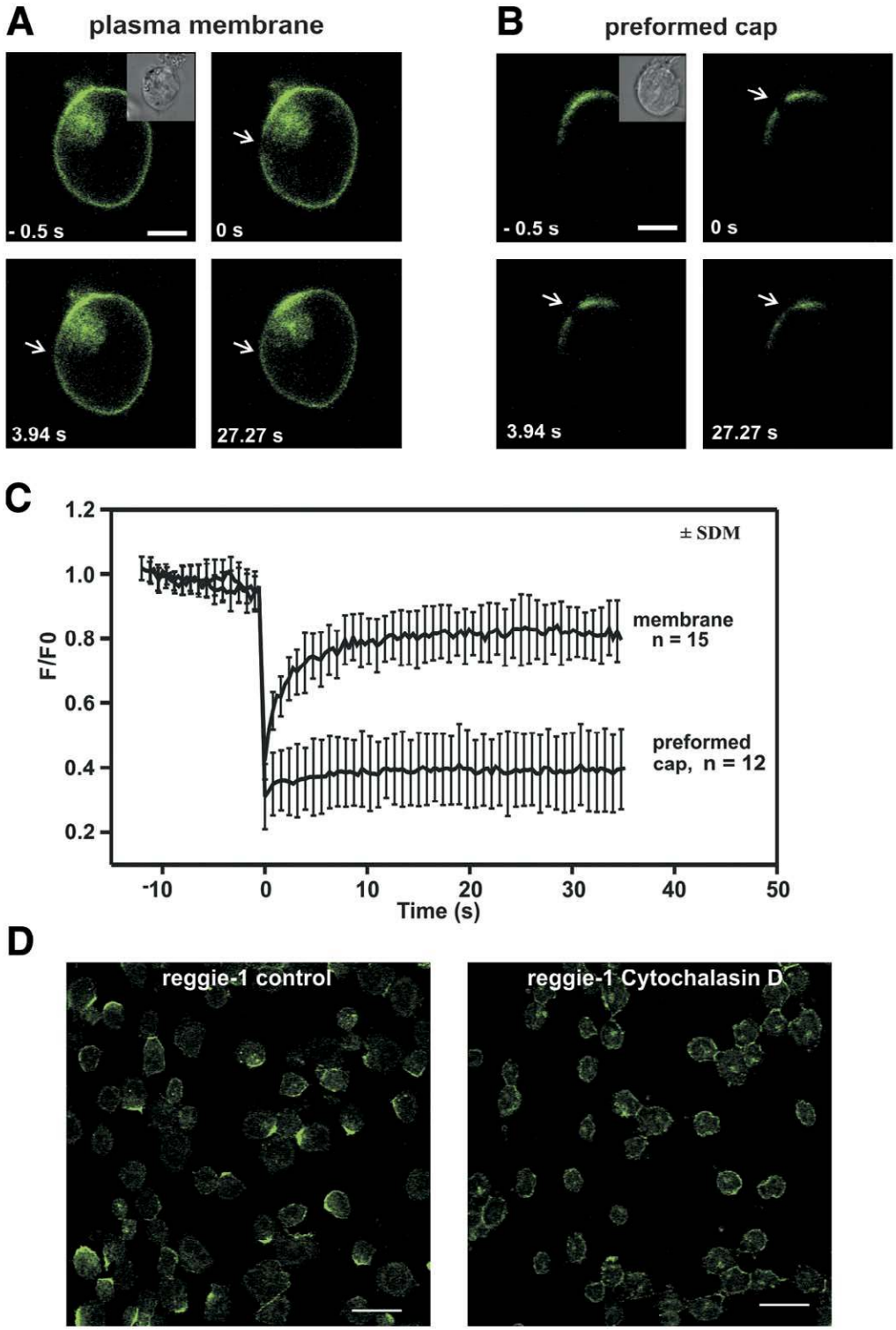

Figure 2. Analysis of the lateral mobility of reggie-1 in Jurkat T cells: ***A, B*)** FRAP analysis of the lateral mobility of reggie-1 (R1FL-EGFP) at the plasma membrane and within the preformed reggie cap in Jurkat T cells. Images of representative cells at key time points are shown, the insets show DIC images of the same cells (arrows indicate the bleached region; scale bar = 5 μm) ***C*)** FRAP tracings averaged from 15 (plasma membrane) or 12 (preformed cap) cells from 5 independent experiments. Note the reduced mobility of reggie-1 in preformed caps. ***D*)** Jurkat T cells were fixed and stained with a mAB against reggie-1, either untreated or treated with 1 μM cytochalasin D. Note the numerous preformed caps in the untreated control, while cytochalasin D treatment resulted in a loss of preformed caps and led to a redistribution of reggie-1 all along the plasma membrane (scale bars = 20 μm)

Fig. 3

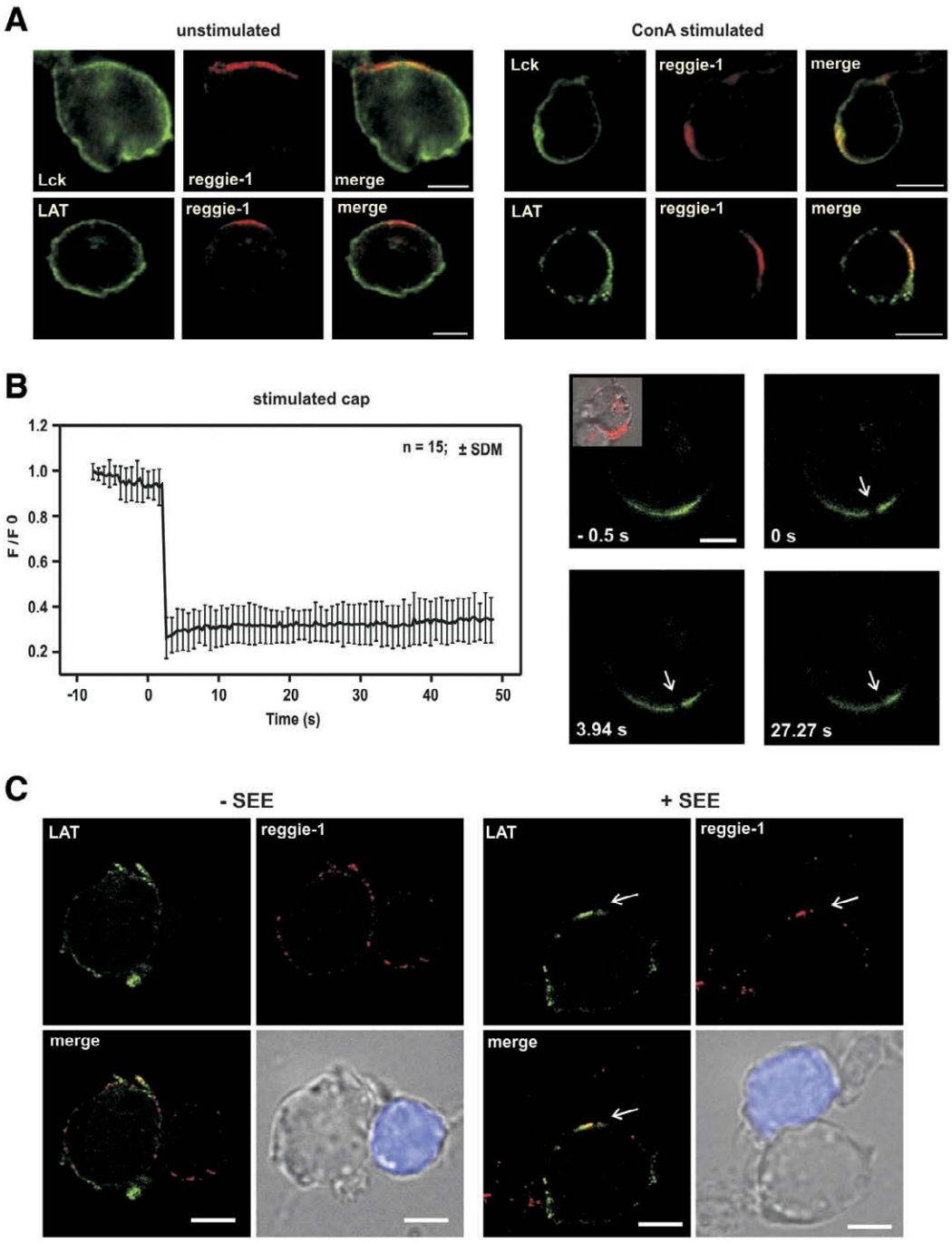

Figure 3. Recruitment of signaling molecules to the reggie caps during T cell stimulation and localization of reggie-1 in the SEE-induced immunological synapse: ***A***) Jurkat T cells, untreated or stimulated with 50 μM concanavalin A, were fixed and stained for reggie-1, lck, and LAT. Note the accumulation of LAT and lck in the region of the reggie cap after stimulation with ConA (scale bar = 5 μm). ***B***) FRAP analysis of the lateral mobility of reggie-1 (R1FL-EGFP) in the cap region after ConA stimulation. Tracings from 15 cells from 5 independent experiments were averaged. Images of a representative cell at key time points are shown, the inset shows an overlay of DIC and ConA fluorescence of the same cell (the bleached region is indicated by arrows; scale bar = 5 μm) ***C***) Accumulation of reggie-1 in SEE-induced immunological synapses. Confocal sections of representative cells from 5 independent experiments stained with antibodies against endogenous LAT and reggie-1 are shown. Raji B lymphocytes were stained with CMAC cell tracker blue and either incubated with 1 μM SEE or left untreated. Note the colocalization and accumulation of reggie-1 and LAT at the Raji B: Jurkat T cell-cell contact after SEE stimulation (scale bars = 5 μm).

Fig. 4

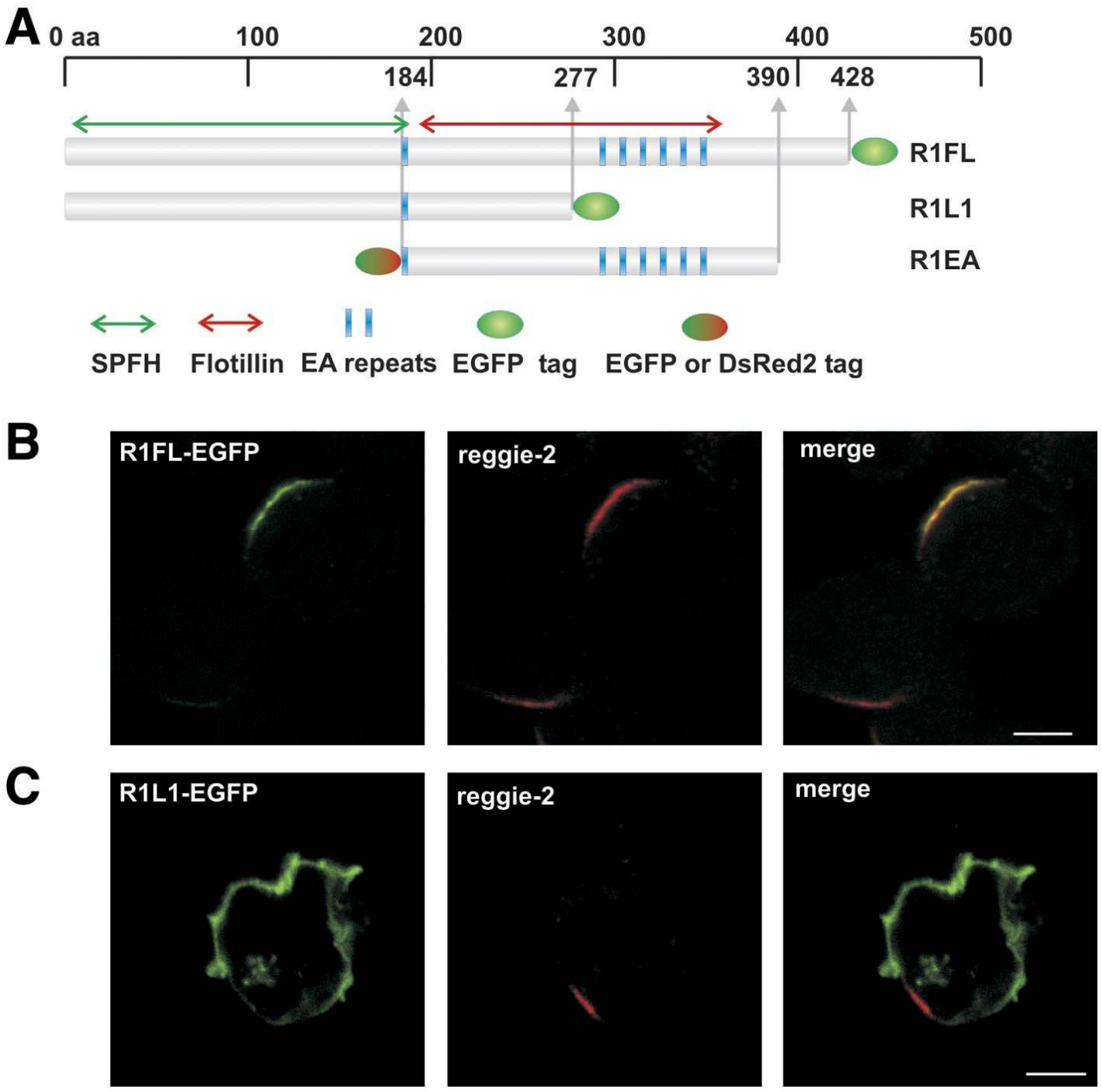

Figure 4. Reggie domains involved in the assembly of preformed caps: ***A***) Schematic representation of reggie-1 mutant constructs; SPFH-, flotillin-domain and EA-repeats, as well as fluorescent proteins used for tagging are indicated. ***B, C***) Localization of R1FL-EGFP and the deletion construct R1L1-EGFP in relation to the preformed reggie cap demarcated by endogenous reggie-2. While R1FL-EGFP accumulates in the reggie cap along with reggie-2, R1L1-EGFP still localizes to the plasma membrane but does not accumulate in the preformed cap (scale bars = 5 µm).

Fig. 5

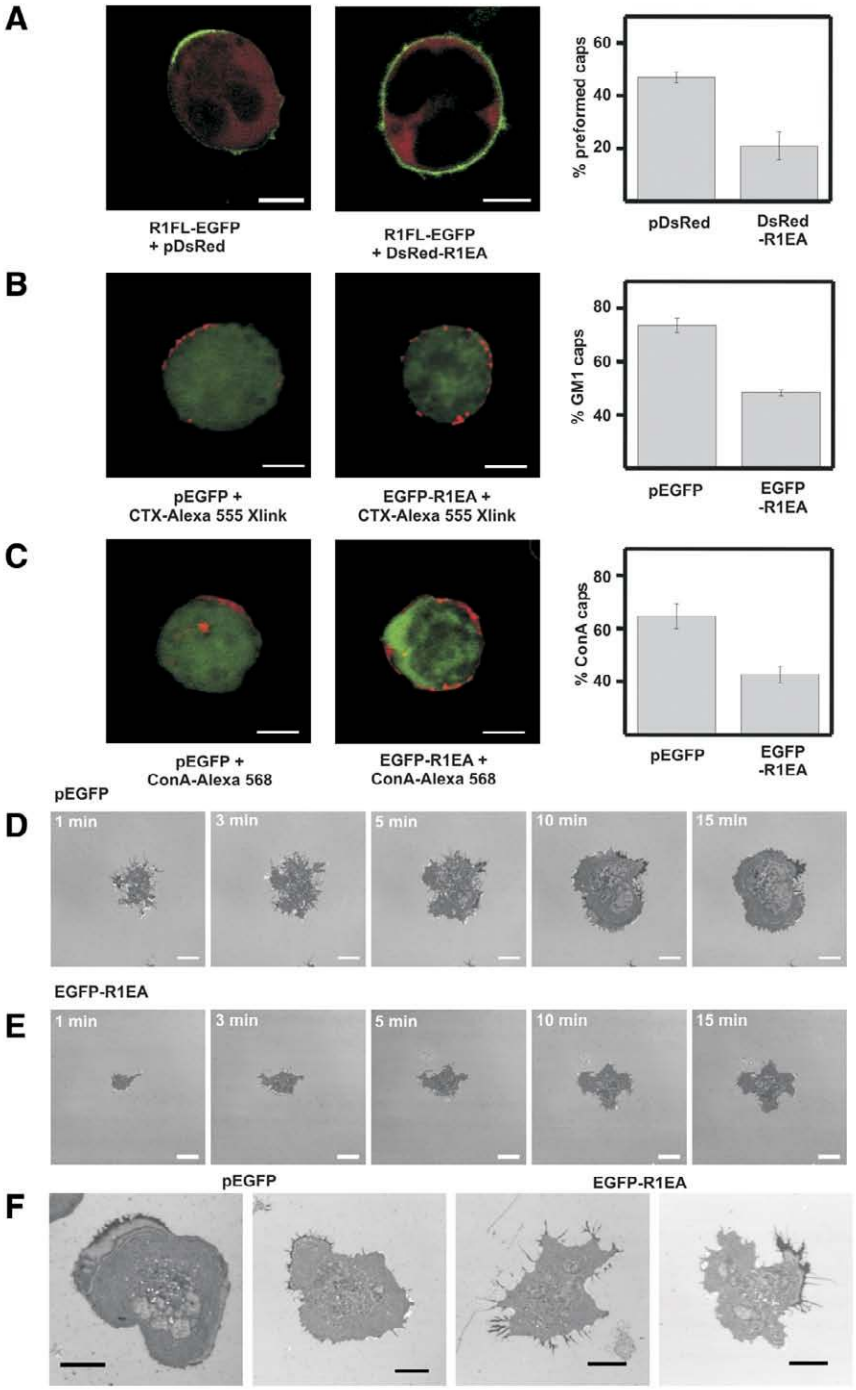

Figure 5. A transnegative mutant inhibits preformed cap assembly and impairs stimulation-induced macrodomain assembly and spreading: ***A)*** Living Jurkat T cells transiently transfected with R1FL-EGFP and either DsRed-R1EA or pDsRed were analyzed by confocal microscopy and the percentage of cells exhibiting a preformed reggie-1 cap was determined. Expression of R1EA significantly reduced the occurrence of preformed reggie caps, so that R1FL-EGFP was evenly distributed around the cell (181 cells from 3 independent experiments were analyzed; scale bars = 5 μm) ***B, C)*** Jurkat T cells transiently transfected with either EGFP-R1EA or pEGFP as a control were stimulated by cross-linking with cholera-toxin B-Alexa 555 or with Concanavalin-Alexa 568. In control cells, cross-linked molecules accumulated in a cap, whereas in R1EA-expressing cells, cross-linked molecules were detected in clusters all around the cell (200 and 150 cells, respectively, from 3 independent experiments were analyzed; scale bars = 5 μm). All error bars indicate the SDM. ***D–F***) IRM images of Jurkat T cells spreading on ConA-coated coverslips. Cells were transiently transfected either with pEGFP as control or with EGFP-R1EA. Note the severely impaired spreading response in cells expressing the EGFP-R1EA mutant (scale bars = 10 μm).

Fig. 6

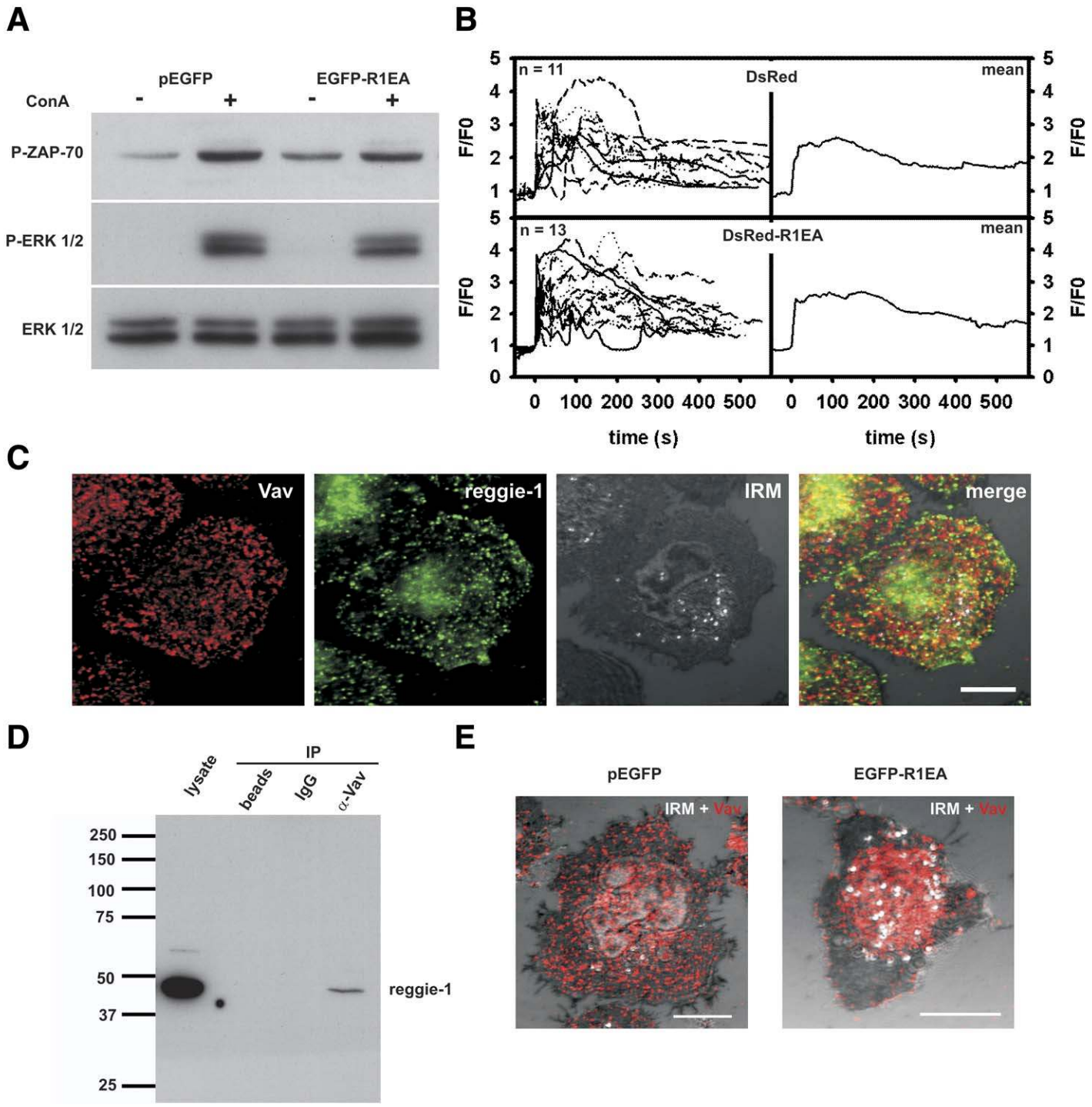

Figure 6. The transnegative reggie mutant impairs Vav localization but does not affect Ca^{2+}-signaling or ERK activation: ***A***) Cells were transiently transfected with pEGFP or EGFP-R1EA, stimulated with ConA and the phosphorylation of ZAP-70 and ERK1/2 were analyzed by Western-blotting using phospho-specific antibodies. Total ERK1/2 is shown as a loading control. ***B***) Ca^{2+} imaging of cells either transfected with R1EA-DsRed or DsRed during spreading on ConA-coated coverslips. Tracings of single cells (***left***) and mean tracings (***right***) are shown. ***C***) Colocalization of endogenous Vav and reggie-1 stained with specific antibodies during spreading on ConA-coated coverslips (scale bar = 10 μm) ***D***) Coimmunoprecipitation of Vav and reggie-1. Precipitation of endogenous Vav reliably coprecipitated endogenous reggie-1 (precipitations with protein A-sepharose alone (beads) and in combination with rabbit IgG are shown as controls). ***E***) Effects of R1EA expression on Vav localization during spreading, merges of IRM and immunofluorescence images are shown (scale bar = 10 μm).